www.sciencemag.org/content/362/6410/eaat5434/suppl/DC1

Supplementary Material for

Saturn's magnetic field revealed by the Cassini Grand Finale

Michele K. Dougherty*, Hao Cao, Krishan K. Khurana, Gregory J. Hunt, Gabrielle Provan, Stephen Kellock, Marcia E. Burton, Thomas A. Burk, Emma J. Bunce, Stanley W. H. Cowley, Margaret G. Kivelson, Christopher T. Russell, David J. Southwood

*Corresponding author. Email: m.dougherty@imperial.ac.uk

Published 5 October 2018, *Science* **362**, eaat5434 (2017)
DOI: 10.1126/science.aat5434

This PDF file includes:

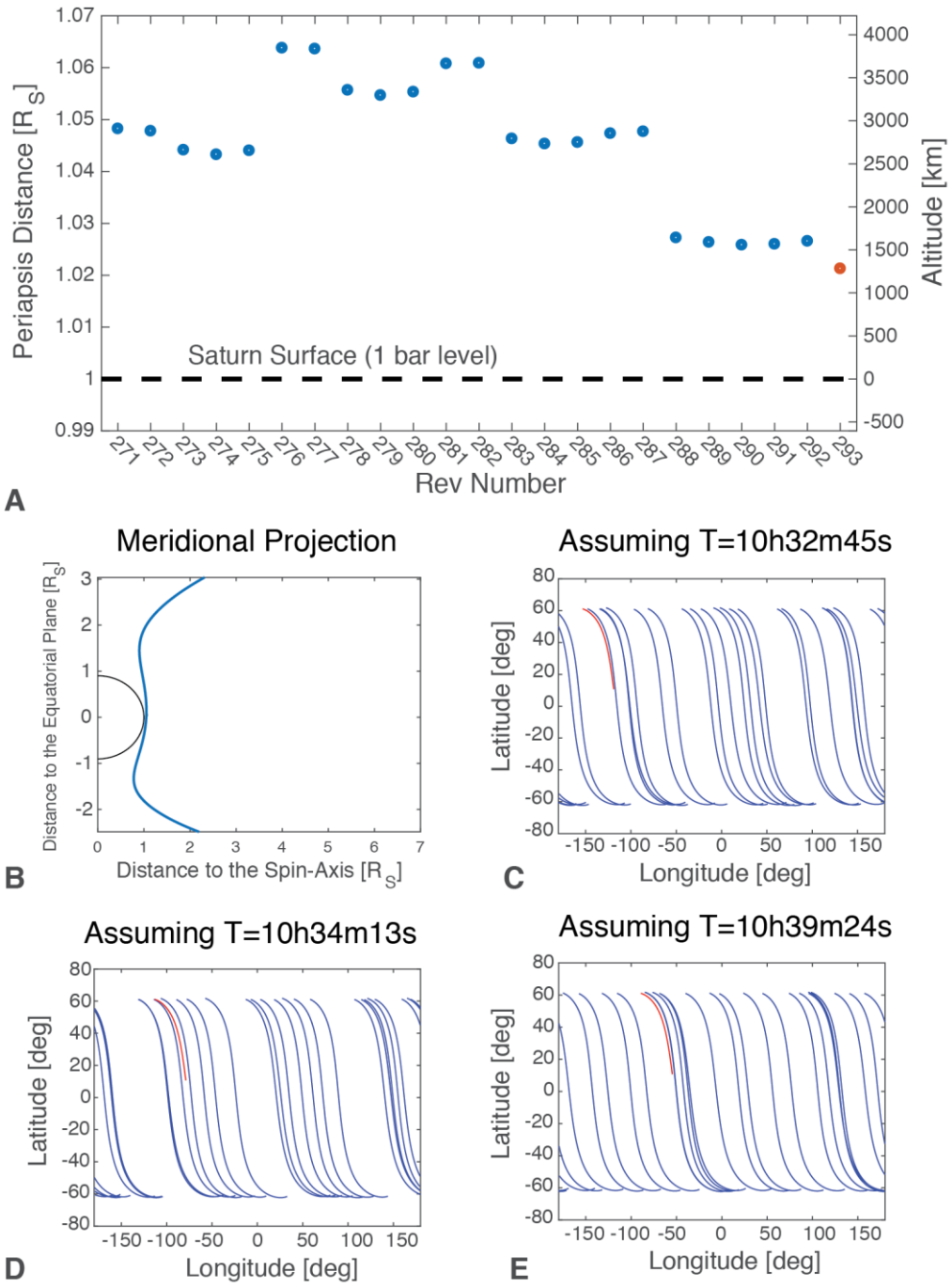

Fig. S1. Characteristics of the trajectory of Cassini Grand Finale orbits. Panel A shows the periapse distance for each orbit. Panel B shows the meridional projection of the first Grand Finale orbit (Rev 271). Panel C-E show and latitude-longitude coverage of the trajectory of the Cassini Grand Finale orbits for three different assumed rotation periods.

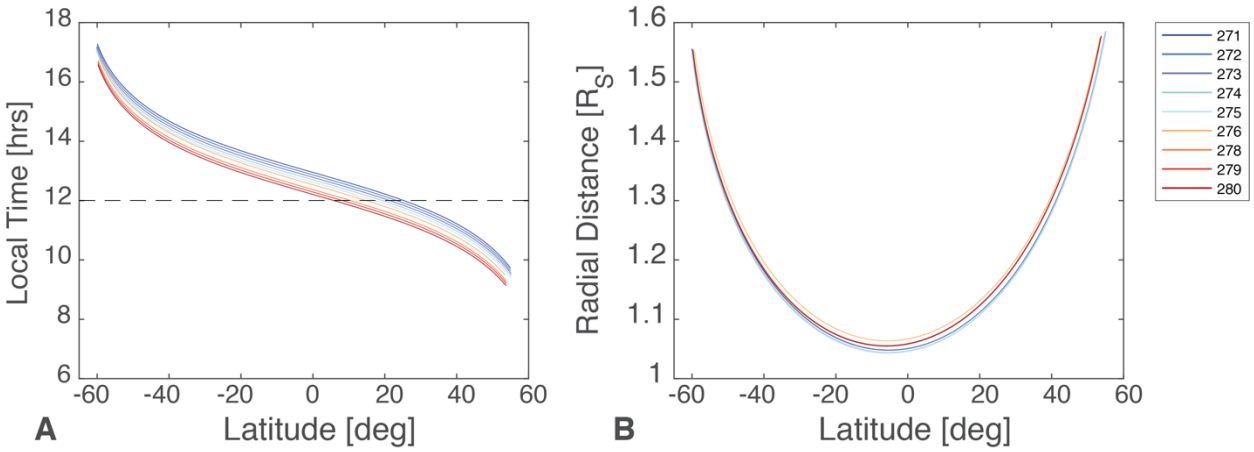

Fig. S2. Characteristics of the trajectory of nine Cassini Grand Finale orbits. Panel A shows local time versus latitude, while panel B shows radial distance versus latitude. The same colour code applies to both panels. We only show the portion of the trajectory when the Cassini magnetometer was in range 3 (magnetic field strength > 10,000 nT). The spacecraft was in the morning (afternoon) sector in the northern (southern) hemisphere.

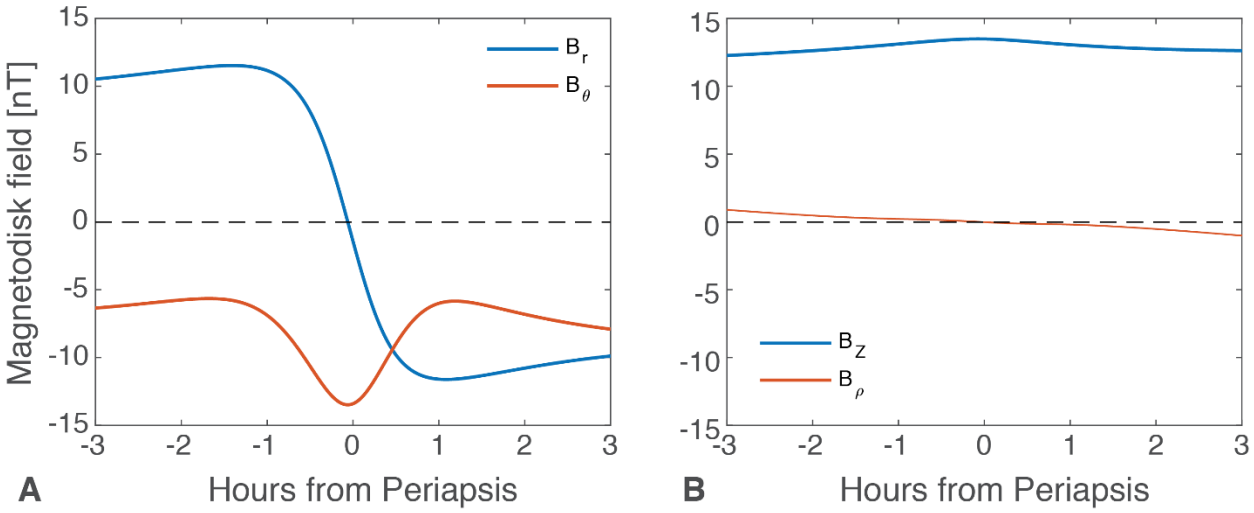

Fig. S3. The expected magnetodisk field along the Cassini Grand Finale orbits. The same field is shown in two different coordinate systems: Saturn-centered spherical coordinates (Panel A) and cylindrical coordinates (Panel B). The trajectory of Cassini Rev 271 was used, and the following parameters for the magnetodisk field model were adopted $(\boldsymbol{a}, \boldsymbol{b}, \boldsymbol{D}, \boldsymbol{\mu_0 I}) = (\boldsymbol{6.5\ R_S}, \boldsymbol{25\ R_S}, \boldsymbol{2.5\ R_S}, \boldsymbol{48.5\ nT})$. See references (*22-26*) for definition of the parameters of the magnetodisk field. It can be seen from the right panel that the magnetodisk field along the ± 3 hours from periapsis of the Cassini Grand Finale trajectory is close to that of a uniform field in the direction parallel to the spin-axis, $\boldsymbol{B_Z}$, around 12 nT. The expected magnetodisk field is very small in the cylindrical radial direction: less than 0.25 nT $\boldsymbol{B_\rho}$ within +/- 1 hour from the periapsis. This makes $\boldsymbol{B_\rho}$ the cleanest component to probe the internal magnetic field of Saturn.

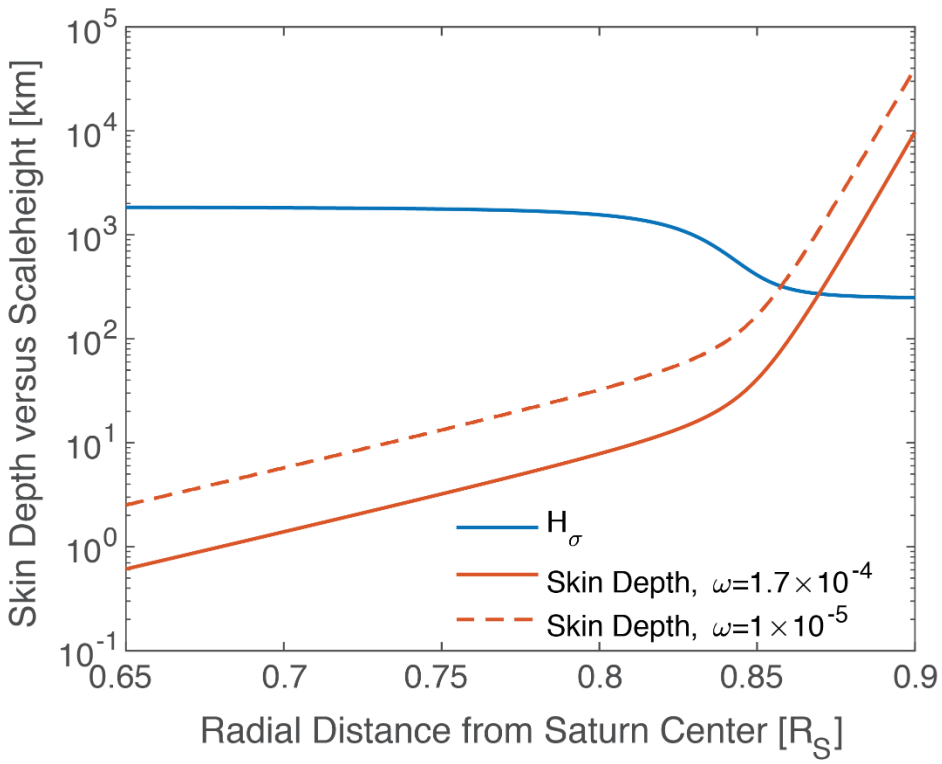

Fig. S4. The frequency dependent electromagnetic (EM) skin depth compared to the electrical conductivity scaleheight inside Saturn. The electrical conductivity profile of *(59)* is adopted for the calculations here. The two frequencies shown here correspond to the rotational frequency of Saturn $\omega_r = \frac{2\pi}{10.5\ hours} \sim 1.7 \times 10^{-4}$ and the orbital period of Cassini Grand Finale orbits $\omega_o = \frac{2\pi}{7\ Earth\ days} \sim 1.0 \times 10^{-5}$. It can be seen that EM induction inside Saturn would occur at depth 0.87 $\boldsymbol{R_S}$ for ω_{ind} equal to the rotational frequency of Saturn and at depth 0.86 $\boldsymbol{R_S}$ for ω_{ind} equal to the orbital period of Cassini Grand Finale orbits.

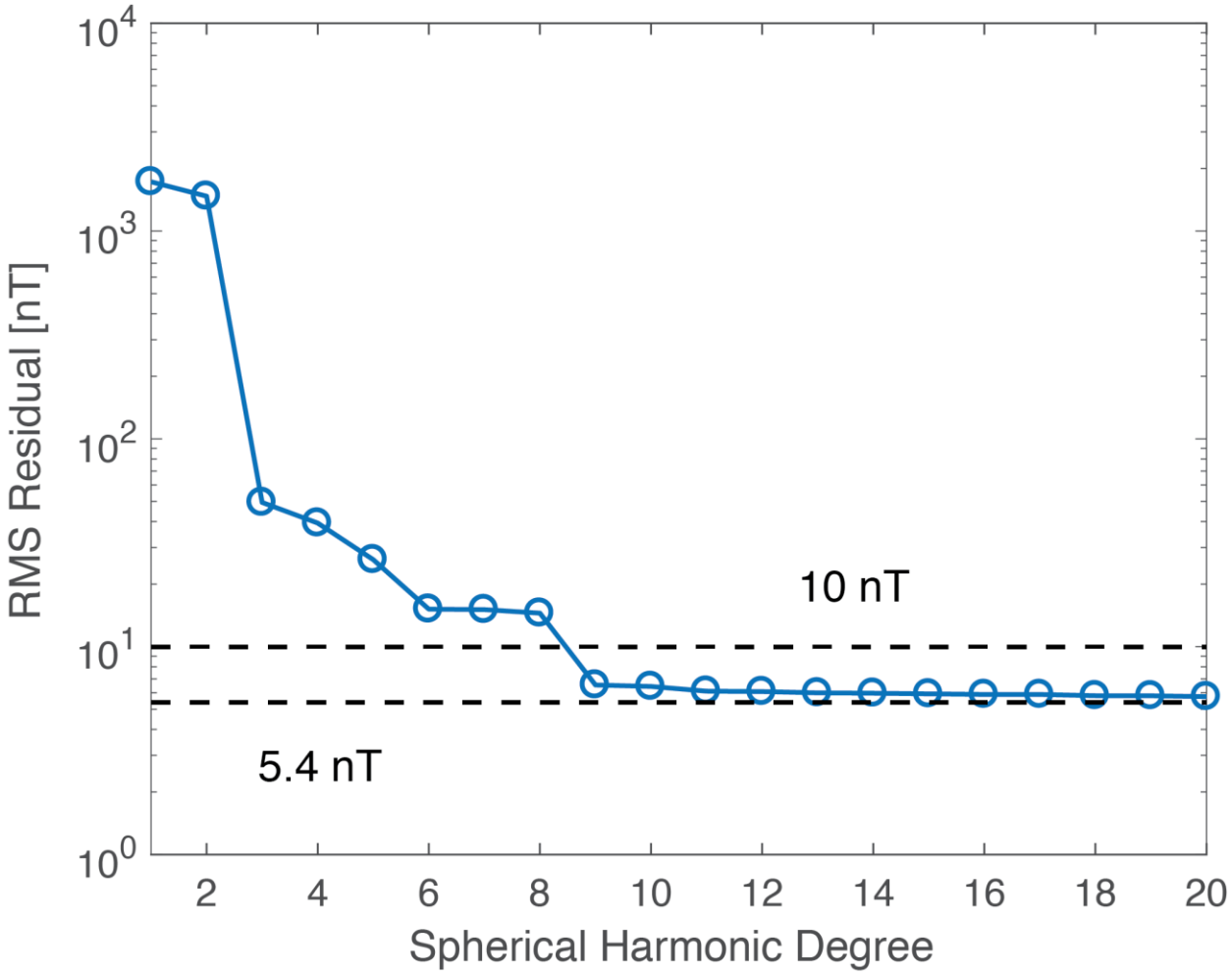

Fig. S5. Root-mean-square (RMS) residual as a function of maximum truncation degree in un-regularized inversion of Saturn's internal magnetic field from Cassini Grand Finale data. A model with Gauss coefficients up to at least spherical harmonic degree 9 is required by the data.

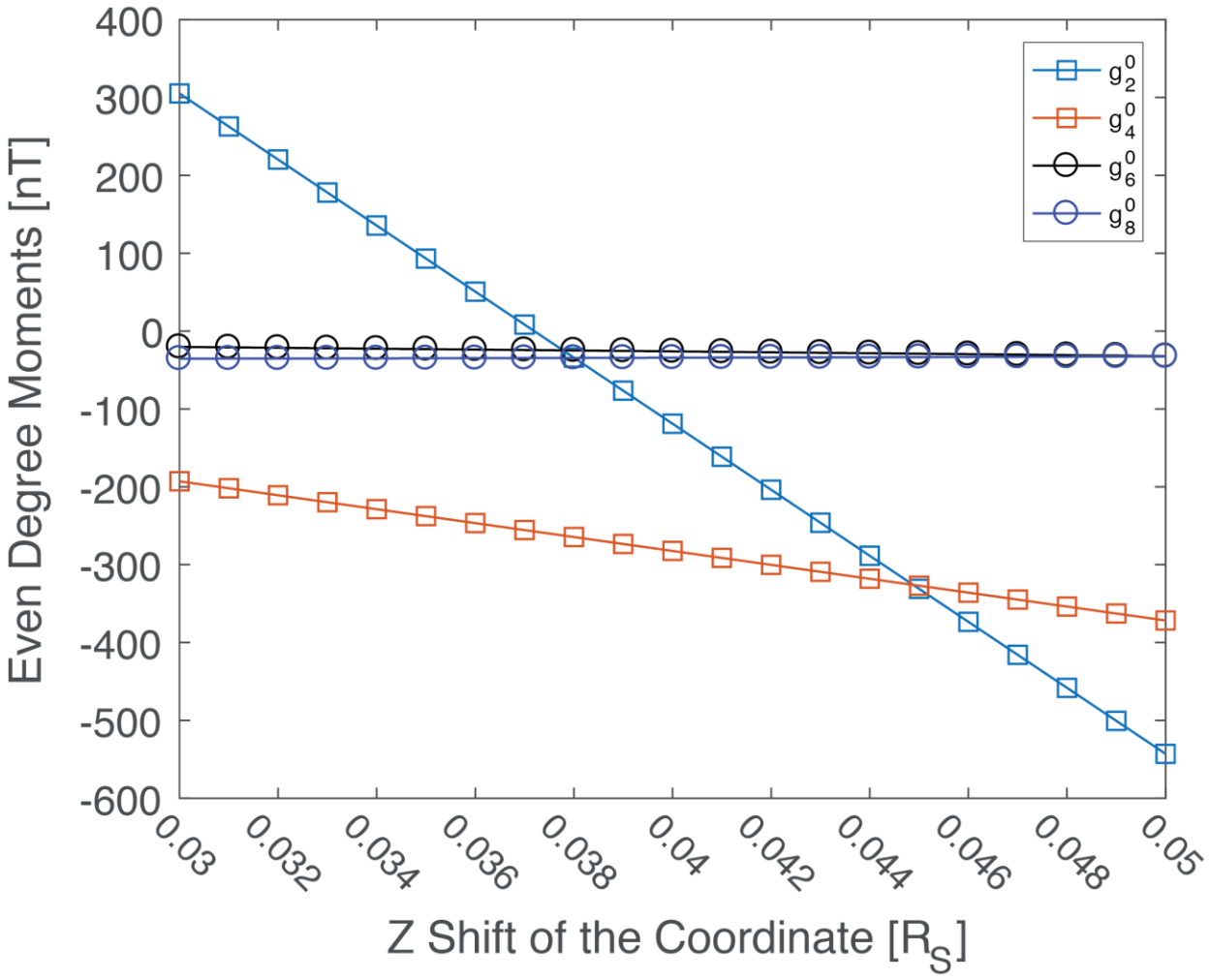

Fig. S6. Gauss coefficients of Saturn's internal magnetic field in Z-shifted coordinates. Only the quadrupole coefficients g_2^0 becomes zero in a coordinate shifted northward by about 0.037 R_S, all other even-degree moments g_4^0, g_6^0, g_8^0 remain non-zero. In addition, g_4^0 becomes more than an order of magnitude larger in these shifted coordinates compared to that in the Saturn-centered coordinates.

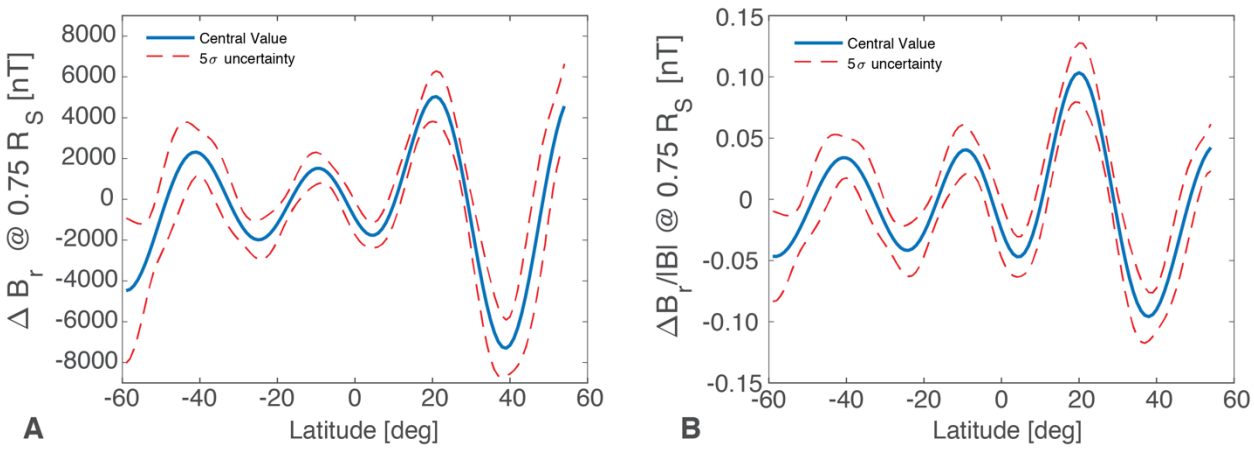

Fig. S7. Small-scale axisymmetric magnetic field of Saturn at 0.75 R_S. Panel A shows ΔB_r while panel B shows $\Delta B_r/|B|$. The central value of ΔB_r is computed using the central values of the degree 4 to 11 Gauss coefficients of the Cassini 11 model and value of $|B| = \sqrt{B_r^2 + B_\theta^2}$ is computed using the central values of the degree 1 to 3 Gauss coefficients of the Cassini 11 model. The uncertainties are computed using the full covariance matrix up to degree 14. The small-scale magnetic perturbations are on the order of 5-10% of the local background field.

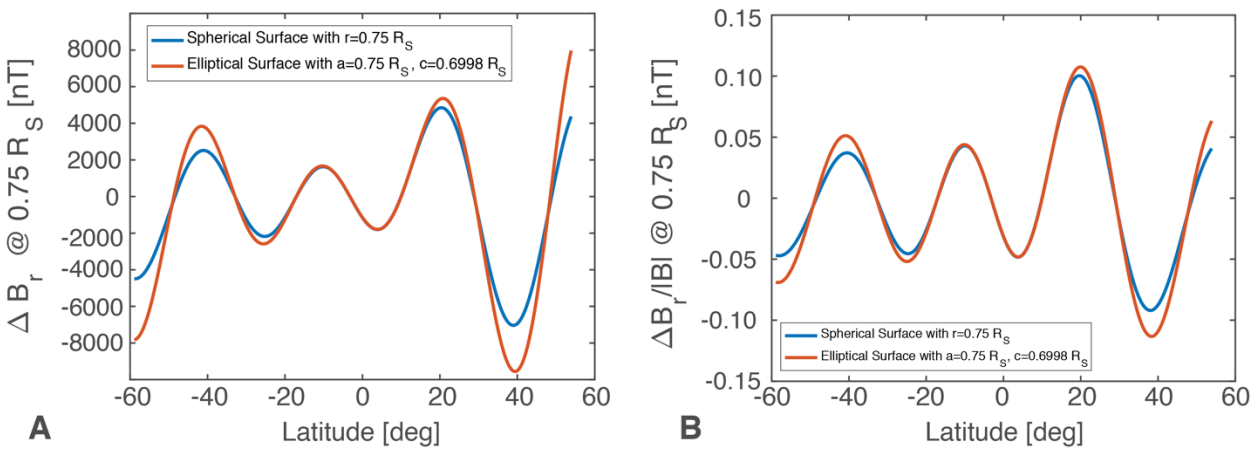

Fig. S8. Small-scale axisymmetric magnetic field of Saturn on a spherical surface with radius 0.75 R_S and on a dynamically flattened elliptical surface with equatorial radius 0.75 R_S and polar radius 0.6998 R_S. Panel A shows ΔB_r while panel B shows $\Delta B_r/|B|$. The central value of ΔB_r is computed using the central values of the degree 4 to 11 Gauss coefficients of the Cassini 11 model and the value of $|B| = \sqrt{B_r^2 + B_\theta^2}$ is computed using the central values of the degree 1 to 3 Gauss coefficients of the Cassini 11 model. It can be seen that the small-scale magnetic field are broadly similar on the spherical and dynamically flattened elliptical surface.

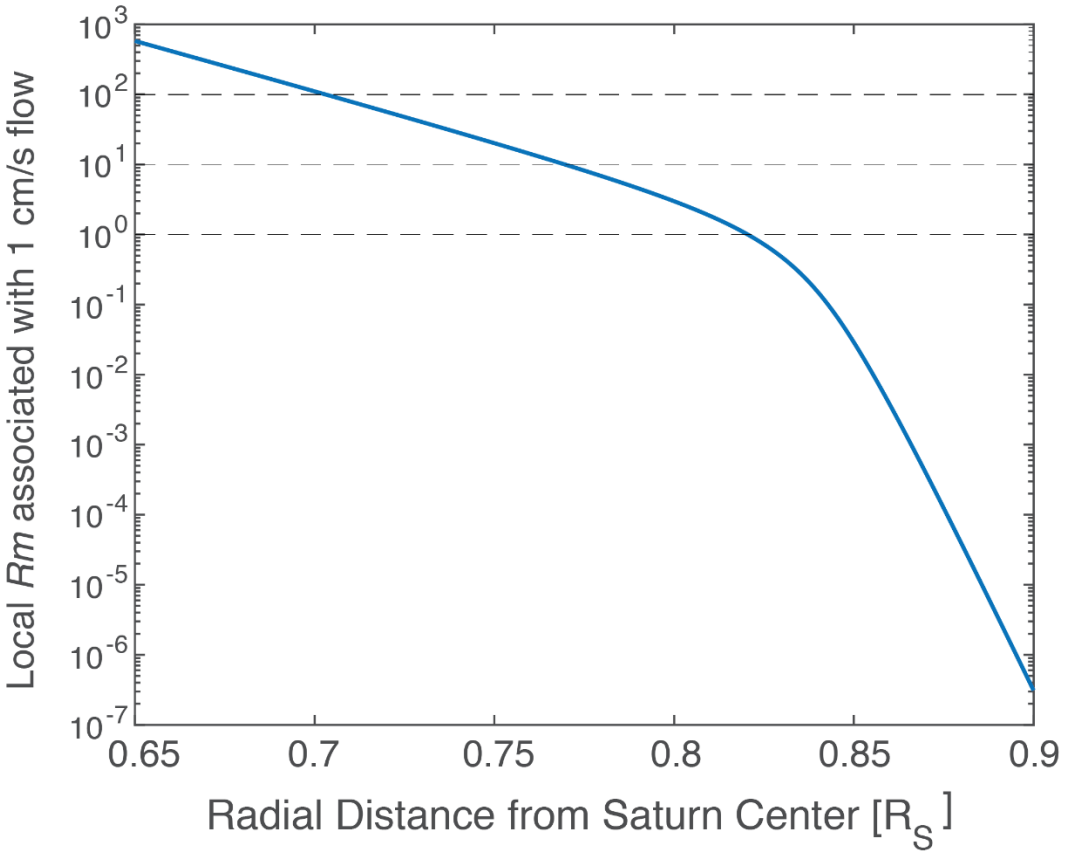

Fig. S9. Local magnetic Reynolds number inside Saturn assuming 1 cm/s flow and the electrical conductivity profile of *(59)*.

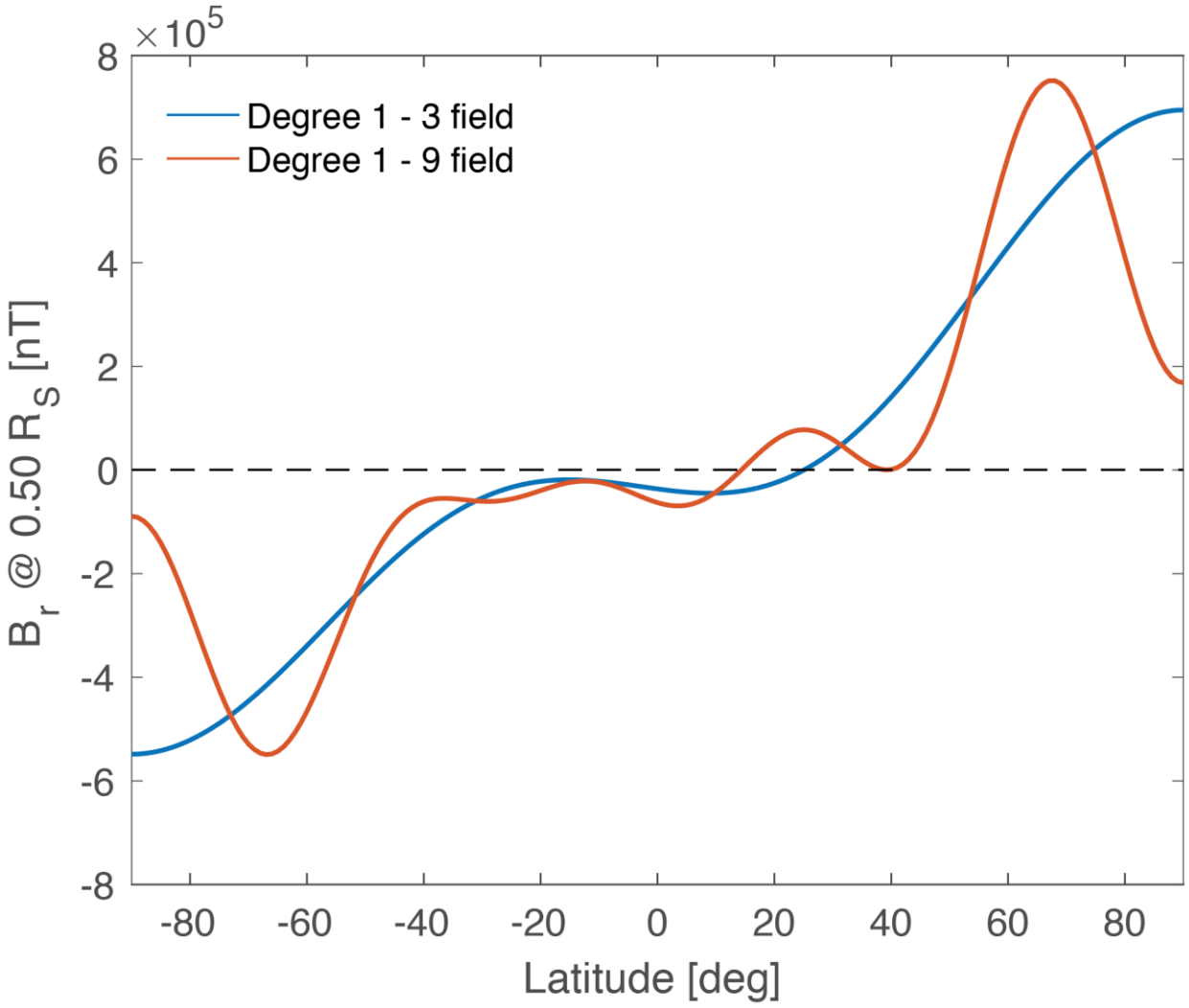

Fig. S10. Saturn's internal magnetic field evaluated at 0.50 R_S. The blue profile is computed from the degree 1 to degree 3 Gauss coefficients while the red profile is computed from the degree 1 to degree 9 Gauss coefficients of the Cassini 11 model (Table 1).

	Un-regularized degree 3 [nT]	Un-regularized degree 6 [nT]
g_1^0	21122	21156
g_2^0	1524	1591
g_3^0	2218	2296
g_4^0		115
g_5^0		74
g_6^0		49
RMS Residual	49.4	15.2

Table S1. Gauss Coefficients of unregularized internal field models with different truncation degree.

	Inner edge $a\ [R_S]$	Outer edge $b\ [R_S]$	Half thickness $D\ [R_S]$	$\mu_0 I$ $[nT]$
Nominal model	6.5	20	2.5	40
Rev 271	6.5	25	2.5	48.8
Rev 272	6.5	25	2.5	42.5
Rev 273	6.5	25	2.5	48.24
Rev 274	6.5	25	2.5	45.1
Rev 275	6.5	25	2.5	52
Rev 276	6.5	25	2.5	60
Rev 278	6.5	25	2.5	49.7
Rev 279	6.5	25	2.5	58.1
Rev 280	6.5	25	2.5	29.9

Table S2. Coefficients of the magnetodisk field model derived for each orbit.

References and Notes

1. D. J. Stevenson, Planetary magnetic fields. *Earth Planet. Sci. Lett.* **208**, 1–11 (2003). doi:10.1016/S0012-821X(02)01126-3

2. E. J. Smith, L. Davis Jr., D. E. Jones, P. J. Coleman Jr., D. S. Colburn, P. Dyal, C. P. Sonett, Saturn's magnetic field and magnetosphere. *Science* **207**, 407–410 (1980). doi:10.1126/science.207.4429.407 Medline

3. M. H. Acuña, N. F. Ness, The magnetic field of saturn: Pioneer 11 observations. *Science* **207**, 444–446 (1980). doi:10.1126/science.207.4429.444 Medline

4. J. E. P. Connerney, N. F. Ness, M. H. Acunã, Zonal harmonic model of Saturn's magnetic field from Voyager 1 and 2 observations. *Nature* **298**, 44–46 (1982). doi:10.1038/298044a0

5. J. E. P. Connerney, M. H. Acunã, N. F. Ness, The Z3 model of Saturn's magnetic field and the Pioneer 11 vector helium magnetometer observations. *J. Geophys. Res.* **89** (A9), 7541–7544 (1984). doi:10.1029/JA089iA09p07541

6. L. Davis Jr., E. J. Smith, New models of Saturn's magnetic field using Pioneer 11 Vector Helium Magnetometer data. *J. Geophys. Res.* **91** (A2), 1373–1380 (1986). doi:10.1029/JA091iA02p01373

7. L. Davis Jr., E. J. Smith, A model of Saturn's magnetic field based on all available data. *J. Geophys. Res.* **95** (A9), 15257–15261 (1990). doi:10.1029/JA095iA09p15257

8. M. K. Dougherty, S. Kellock, D. J. Southwood, A. Balogh, E. J. Smith, B. T. Tsurutani, B. Gerlach, K.-H. Glassmeier, F. Gleim, C. T. Russell, G. Erdos, F. M. Neubauer, S. W. H. Cowley, The Cassini magnetic field investigation. *Space Sci. Rev.* **114**, 331–383 (2004). doi:10.1007/s11214-004-1432-2

9. M. K. Dougherty, N. Achilleos, N. Andre, C. S. Arridge, A. Balogh, C. Bertucci, M. E. Burton, S. W. H. Cowley, G. Erdos, G. Giampieri, K.-H. Glassmeier, K. K. Khurana, J. Leisner, F. M. Neubauer, C. T. Russell, E. J. Smith, D. J. Southwood, B. T. Tsurutani, Cassini magnetometer observations during Saturn orbit insertion. *Science* **307**, 1266–1270 (2005). doi:10.1126/science.1106098 Medline

10. M. E. Burton, M. K. Dougherty, C. T. Russell, Models of Saturn's internal planetary magnetic field based on Cassini observations. *Planet. Space Sci.* **57**, 1706–1713 (2009). doi:10.1016/j.pss.2009.04.008

11. H. Cao, C. T. Russell, U. R. Christensen, M. K. Dougherty, M. E. Burton, Saturn's very axisymmetric magnetic field: No detectable secular variation or tilt. *Earth Planet. Sci. Lett.* **304**, 22–28 (2011). doi:10.1016/j.epsl.2011.02.035

12. H. Cao, C. T. Russell, J. Wicht, U. R. Christensen, M. K. Dougherty, Saturn's high degree magnetic moments: Evidence for a unqiue planetary dynamo. *Icarus* **221**, 388–394 (2012). doi:10.1016/j.icarus.2012.08.007

13. S. T. Weir, A. C. Mitchell, W. J. Nellis, Metallization of fluid molecular hydrogen at 140 GPa (1.4 Mbar). *Phys. Rev. Lett.* **76**, 1860–1863 (1996). doi:10.1103/PhysRevLett.76.1860 Medline

14. M. Zaghoo, I. F. Silvera, Conductivity and dissociation in liquid metallic hydrogen and implications for planetary interiors. *Proc. Natl. Acad. Sci. U.S.A.* **114**, 11873–11877 (2017). doi:10.1073/pnas.1707918114 Medline

15. E. N. Parker, Hydromagnetic dynamo models. *Astrophys. J.* **122**, 293 (1955). doi:10.1086/146087

16. F. Krause, K.-H. Rädler, *Mean-Field Magnetohydrodynamics and Dynamo Theory* (Pergamon, 1980).

17. H. K. Moffatt, *Magnetic Field Generation in Electrically Conducting Fluids* (Cambridge Univ. Press, 1978).

18. T. G. Cowling, The magnetic field of sunspots. *Mon. Not. R. Astron. Soc.* **94**, 39–48 (1933). doi:10.1093/mnras/94.1.39

19. P. Charbonneau, *Solar and Stellar Dynamos: Saas-Fee Advanced Course 39 Swiss Society for Astrophysics and Astronomy* (Springer-Verlag Berlin Heidelberg, 2013).

20. H. Cao, D. J. Stevenson, Zonal flow magnetic field interaction in the semi-conducting region of giant planets. *Icarus* **296**, 59–72 (2017). doi:10.1016/j.icarus.2017.05.015

21. D. J. Southwood, M. K. Dougherty, A. Balogh, S. W. H. Cowley, E. J. Smith, B. T. Tsurutani, C. T. Russell, G. L. Siscoe, G. Erdos, K.-H. Glassmeier, F. Gleim, F. M. Neubauer, Magnetometer measurements from the Cassini Earth swing-by. *J. Geophys. Res.* **106** (A12), 30109–30128 (2001). doi:10.1029/2001JA900110

22. E. J. Bunce, S. W. H. Cowley, I. I. Alexeev, C. S. Arridge, M. K. Dougherty, J. D. Nichols, C. T. Russell, Cassini observations of the variation of Saturn's ring current parameters with system size. *J. Geophys. Res.* **112** (A10), A10202 (2007). doi:10.1029/2007JA012275

23. J. E. P. Connerney, M. H. Acunã, N. F. Ness, Saturn's ring current and inner magnetosphere. *Nature* **292**, 724–726 (1981). doi:10.1038/292724a0

24. J. E. P. Connerney, M. H. Acunã, N. F. Ness, Currents in Saturn's magnetosphere. *J. Geophys. Res.* **88** (A11), 8779–8789 (1983). doi:10.1029/JA088iA11p08779

25. G. Giampieri, M. Dougherty, Modeling of the ring current in Saturn's magnetosphere. *Ann. Geophys.* **22**, 653–659 (2004). doi:10.5194/angeo-22-653-2004

26. T. M. Edwards, E. J. Bunce, S. W. H. Cowley, A note on the vector potential of Connerney et al.'s model of the equatorial current sheet in Jupiter's magnetosphere. *Planet. Space Sci.* **49**, 1115–1123 (2001). doi:10.1016/S0032-0633(00)00164-1

27. J. F. Carbary, D. G. Mitchell, Periodicities in Saturn's magnetosphere. *Rev. Geophys.* **51**, 1–30 (2013). doi:10.1002/rog.20006

28. D. J. Southwood, S. W. H. Cowley, The origin of Saturn magnetic periodicities: Northern and southern current systems. *J. Geophys. Res.* **119**, 1563–1571 (2014). doi:10.1002/2013JA019632

29. D. A. Gurnett, A. Lecacheux, W. S. Kurth, A. M. Persoon, J. B. Groene, L. Lamy, P. Zarka, J. F. Carbary, Discovery of a north-south asymmetry in Saturn's radio rotation period. *Geophys. Res. Lett.* **36**, L16102 (2009). doi:10.1029/2009GL039621

30. D. J. Andrews, A. J. Coates, S. W. H. Cowley, M. K. Dougherty, L. Lamy, G. Provan, P. Zarka, Magnetospheric period oscillations at Saturn: Comparison of equatorial and high latitude magnetic field periods with north and south Saturn kilometric radiation periods. *J. Geophys. Res.* **115**, 1363 (2010). doi:10.1029/2010JA015666

31. D. J. Southwood, Direct evidence of differences in magnetic rotation rate between Saturn's northern and southern polar regions. *J. Geophys. Res.* **116** (A1), 1–11 (2011). doi:10.1029/2010JA016070

32. G. J. Hunt, G. Provan, S. W. H. Cowley, M. K. Dougherty, D. J. Southwood, Saturn's planetary period oscillations during the closest approach of Cassini's ring-grazing orbits. *Geophys. Res. Lett.* **45**, 4692–4700 (2018). doi:10.1029/2018GL077925

33. G. Provan, S. W. H. Cowley, T. J. Bradley, E. J. Bunce, G. J. Hunt, M. K. Dougherty, Planetary period oscillations in Saturn's magnetosphere: Cassini magnetic field observations over the northern summer solstice interval. *J. Geophys. Res. Space Phys.* **123**, 3859–3899 (2018). doi:10.1029/2018JA025237

34. P. Galopeau, A. Lecacheux, Variations of Saturn's radio rotation period measured at kilometer wavelengths. *J. Geophys. Res.* **105** (A6), 13089–13101 (2000). doi:10.1029/1999JA005089

35. D. A. Gurnett, J. B. Groene, A. M. Persoon, J. D. Menietti, S.-Y. Ye, W. S. Kurth, R. J. MacDowall, A. Lecacheux, The reversal of the rotational modulation rates of the north and south components of Saturn kilometric radiation near equinox. *Geophys. Res. Lett.* **37**, L24101 (2010). doi:10.1029/2010GL045796

36. G. Provan, S. W. H. Cowley, L. Lamy, E. J. Bunce, G. J. Hunt, P. Zarka, M. K. Dougherty, Planetary period oscillations in Saturn's magnetosphere: Coalescence and reversal of northern and southern periods in late northern spring. *J. Geophys. Res.* **121**, 9829–9862 (2016). doi:10.1002/2016JA023056

37. X. Jia, M. G. Kivelson, T. I. Gombosi, Driving Saturn's magnetospheric periodicities from the upper atmosphere/ionosphere. *J. Geophys. Res.* **117** (A04215), 1460 (2012). 10.1029/2011JA017367

38. X. Jia, M. G. Kivelson, Driving Saturn's magnetospheric periodicities from the upper atmosphere/ionosphere: Magnetotail response to dual sources. *J. Geophys. Res.* **117**, A11219 (2012). 10.1029/2012JA018183

39. J. D. Anderson, G. Schubert, Saturn's gravitational field, internal rotation, and interior structure. *Science* **317**, 1384–1387 (2007). doi:10.1126/science.1144835 Medline

40. P. L. Read, T. E. Dowling, G. Schubert, Saturn's rotation period from its atmospheric planetary-wave configuration. *Nature* **460**, 608–610 (2009). doi:10.1038/nature08194

41. R. Helled, E. Galanti, Y. Kaspi, Saturn's fast spin determined from its gravitational field and oblateness. *Nature* **520**, 202–204 (2015). doi:10.1038/nature14278 Medline

42. S. W. H. Cowley, E. J. Bunce, J. M. O'Rourke, A simple quantitative model of plasma flows and currents in Saturn's polar ionosphere. *J. Geophys. Res.* **109** (A5), A05212 (2004). doi:10.1029/2003JA010375

43. G. J. Hunt, S. W. H. Cowley, G. Provan, E. J. Bunce, I. I. Alexeev, E. S. Belenkaya, V. V. Kalegaev, M. K. Dougherty, A. J. Coates, Field-aligned currents in Saturn's southern nightside magnetosphere: Sub-corotation and planetary period oscillation components. *J. Geophys. Res.* **119**, 9847–9899 (2014). doi:10.1002/2014JA020506

44. G. J. Hunt, S. W. H. Cowley, G. Provan, E. J. Bunce, I. I. Alexeev, E. S. Belenkaya, V. V. Kalegaev, M. K. Dougherty, A. J. Coates, Field-aligned currents in Saturn's northern nightside magnetosphere: Evidence for inter-hemispheric current flow associated with planetary period oscillations. *J. Geophys. Res.* **120**, 7552–7584 (2015). doi:10.1002/2015JA021454

45. B. A. Archinal, C. H. Acton, M. F. A'Hearn, A. Conrad, G. J. Consolmagno, T. Duxbury, D. Hestroffer, J. L. Hilton, R. L. Kirk, S. A. Klioner, D. McCarthy, K. Meech, J. Oberst, J. Ping, P. K. Seidelmann, D. J. Tholen, P. C. Thomas, I. P. Williams, Report of the IAU Working Group on Cartographic Coordinates and Rotational Elements: 2015. *Celestial Mech. Dyn. Astron.* **130**, 22 (2018). doi:10.1007/s10569-017-9805-5

46. G. J. Hunt, G. Provan, E. J. Bunce, S. W. H. Cowley, M. K. Dougherty, D. J. Southwood, Field-aligned currents in Saturn's magnetosphere: Observations from the F-ring orbits. *J. Geophys. Res. Space Phys.* **123**, 3806–3821 (2018). doi:10.1029/2017JA025067

47. K. K. Khurana, M. K. Dougherty, G. Provan, G. J. Hunt, M. G. Kivelson, S. W. H. Cowley, D. J. Southwood, C. T. Russell, Discovery of atmospheric-wind-driven electric currents in Saturn's magnetosphere in the gap between Saturn and its rings. *Geophys. Res. Lett.* (2018). 10.1029/2018GL078256

48. M. E. Burton, M. K. Dougherty, C. T. Russell, Saturn's internal planetary magnetic field. *Geophys. Res. Lett.* **37**, L24105 (2010). doi:10.1029/2010GL045148

49. D. J. Stevenson, Saturn's luminosity and magnetism. *Science* **208**, 746–748 (1980). doi:10.1126/science.208.4445.746 Medline

50. D. J. Stevenson, Reducing the non-axisymmetry of a planetary dynamo and an application to Saturn. *Geophys. Astrophys. Fluid Dyn.* **21**, 113–127 (1982). doi:10.1080/03091928208209008

51. U. R. Christensen, J. Wicht, Models of magnetic field generation in partly stable planetary cores: Application to Mercury and Saturn. *Icarus* **196**, 16–34 (2008). doi:10.1016/j.icarus.2008.02.013

52. S. Stanley, A dynamo model for axisymmetrizing Saturn's magnetic field. *Geophys. Res. Lett.* **37**, L05201 (2010). doi:10.1029/2009GL041752

53. D. Gubbins, *Time Series Analysis and Inverse Theory for Geophysicists* (Cambridge Univ. Press, 2004).

54. R. Holme, J. Bloxham, The magnetic fields of Uranus and Neptune: Methods and models. *J. Geophys. Res.* **101**, 2177–2200 (1996). doi:10.1029/95JE03437

55. P. Mauersberger, Das Mittel der energiedichte des geomagnetischen Hauptfeldes an der erdoberflasähe und seine säkulare Änderung. *Gerlands Beitr. Geophys.* **65**, 207–215 (1956).

56. F. J. Lowes, Mean-square values on sphere of spherical harmonic vector fields. *J. Geophys. Res.* **71**, 2179–2179 (1966). doi:10.1029/JZ071i008p02179

57. F. J. Lowes, Spatial power spectrum of the main geomagnetic field, and extrapolation to the core. *Geophys. J. Int.* **36**, 717–730 (1974). doi:10.1111/j.1365-246X.1974.tb00622.x

58. J. J. Liu, P. M. Goldreich, D. J. Stevenson, Constraints on deep-seated zonal winds inside Jupiter and Saturn. *Icarus* **196**, 653–664 (2008). doi:10.1016/j.icarus.2007.11.036

59. The local magnetic Reynolds number is defined as $R_m = U_{conv}H_\sigma/\lambda$, where U_{conv} is the typical convective velocity; λ is the magnetic diffusivity, defined as the inverse of the product of electrical conductivity and magnetic permeability; and H_σ is the conductivity scale-height defined as $H_\sigma = \sigma/|d\sigma/dr|$.

60. U. R. Christensen, Dynamo scaling laws and application to the planets. *Space Sci. Rev.* **152**, 565–590 (2010). doi:10.1007/s11214-009-9553-2

61. T. Gastine, J. Wicht, L. D. V. Duarte, M. Heimpel, A. Becker, Explaining Jupiter's magnetic field and equatorial jet dynamics. *Geophys. Res. Lett.* **41**, 5410–5419 (2014). doi:10.1002/2014GL060814

62. G. A. Glatzmaier, Computer simulations of Jupiter's deep internal dynamics help interpret what Juno sees, *Proceedings of the National Academy of Sciences*, 201709125; DOI:10.1073/pnas.1709125115 (2018).

63. Due the divergence free nature of magnetic field, a poloidal-toroidal decomposition of the magnetic field, $\mathbf{B} = \nabla\times(\nabla\times P\mathbf{e}_r) + \nabla\times T\mathbf{e}_r$, is commonly adopted in the dynamo region. The toroidal magnetic field, $\mathbf{B}_T = \nabla\times T\mathbf{e}_r$ has no radial component, and is associated with local electrical currents. The poloidal magnetic field $\mathbf{B}_P = \nabla\times(\nabla\times P\mathbf{e}_r)$ has no azimuthal component if it is axisymmetric.

64. J. E. P. Connerney, M. H. Acuna, N. F. Ness, T. Satoh, New models of Jupiter's magnetic field constrained by the Io flux tube footprint. *J. Geophys. Res.* **103** (A6), 11929–11939 (1998). doi:10.1029/97JA03726

65. Z. J. Yu, H. K. Leinweber, C. T. Russell, Galileo constraints on the secular variation of the Jovian magnetic field. *J. Geophys. Res.* **115** (E3), E03002 (2010). doi:10.1029/2009JE003492

66. V. A. Ridley, R. Holme, Modeling the Jovian magnetic field and its secular variation using all available magnetic field observations. *J. Geophys. Res.* **121**, 309–337 (2016). doi:10.1002/2015JE004951

67. K. M. Moore, J. Bloxham, J. E. P. Connerney, J. L. Jørgensen, J. M. G. Merayo, The analysis of initial Juno magnetometer data using a sparse magnetic field representation. *Geophys. Res. Lett.* **44**, 4687–4693 (2017). doi:10.1002/2017GL073133

68. Assuming 1 cm s^{-1} flow and an electrical conductivity of 2×10^5 S/m, R_m associated with a layer with a thickness of 0.2 R_S would be ~30,000.